LUNDS UNIVERSITET

DEPARTMENT of PSYCHOLOGY

The medial temporal lobe subregional atrophy in early onset and late onset amnestic variant Alzheimer's disease

Wutt Hmon

Master's Thesis (30 hp)

Spring 2021

Supervisor: Mikael Johansson

Laura Wisse

Abstract

Memory impairment and prominent hippocampal atrophy are the most recognisable features of Alzheimer's disease (AD). It has been known that hippocampus and surrounding medial temporal lobe (MTL) structures support memory processes. However, specific function of each MTL subfield remains to be elucidated. Not all MTL subfields are uniformly affected by AD pathology and the spread of AD pathology follows a predictable pattern is closely correlated with atrophy seen on MRI and clinical symptoms. Hence, we propose that studying memory deficits in AD in tandem with MTL subfield atrophy might be fruitful to probe specific contribution of each MTL subfield to memory function. However, both clinical and anatomical heterogeneities have been reported in AD and age of onset is one source of heterogeneity. AD is commonly subdivided into early onset AD (EOAD = age of onset ≤ 65) and late onset AD (LOAD = age of onset > 65) and the two subtypes have several important clinical and anatomical differences. In order to probe the specific function of each MTL subregion by correlating the AD affected subregion and the corresponding cognitive deficit, we need to better characterise the topography of atrophy in AD patients. Therefore, the aim of this study is to investigate whether MTL subregional atrophy in EOAD and LOAD of amnestic type share similar topography. As atrophy patterns become less differentiated in the later stages of AD, in order to observe focal changes during early stages of AD, we also compared MTL subregional atrophy in a group with early onset mild cognitive impairment (EOMCI) and a group with late onset mild cognitive impairment (LOMCI) as mild cognitive impairment stage is proposed to be the precursor stage of AD. We found that all patient groups had varying degree of MTL subregional atrophy. Generally, current study found that differences in MTL subregional atrophy between EOAD and LOAD could be explained by age difference, possible TDP-43 co-pathology and higher tau burden in LOAD.

Keywords: Medial temporal lobe subregional atrophy, Early onset AD vs late onset AD, Amnestic variant of AD

The medial temporal lobe subregional atrophy in early onset and late onset amnesic variant Alzheimer's dementia

Memory impairment is a canonical feature of Alzheimer's dementia (AD) (Tellechea et al., 2018; van der Flier et al., 2011) and hippocampal atrophy is the most conspicuous characteristic of AD (McKhann et al., 1984). Hippocampus and adjacent medial temporal lobe (MTL) structures are long known to support various memory processes (Squire, 2009). However, hippocampus is not a homogenous structure but a conglomeration of functionally distinct but tightly interconnected regions called "subfields" (Small, 2014). The specific contribution of each subfield to memory is not completely known (Travis et al., 2014). Since not all subfields are uniformly vulnerable to AD (La Joie et al., 2013; Mueller et al., 2017), selective vulnerability of subfields in can be delineated from structural magnetic resonance imaging (MRI) (Iglesias et al., 2015). Studying memory loss in AD in tandem with selectively atrophied subfields could offer insight into neural correlates of specific memory sub-functions. Therefore, our research interest is to characterise atrophy pattern in typical amnestic AD.

The importance of hippocampus for memory was first realised when surgical removal of hippocampus left patient HM with permanent loss of ability of form new episodic memories (Squire, 2009). Since then, hippocampus has been the most actively researched brain region and it has been associated with various memory subtypes and mnemonic processes including but not limited to episodic, associative, contextual memory as well as encoding, binding, pattern separation, consolidation, recollection and inferential processes (Genon et al., 2018). However, hippocampus is not the only structure that supports memory function and it is in fact, a part of the MTL memory system which encompasses hippocampus and surrounding structures in the para hippocampal gyrus, namely: perirhinal cortex (PRC: Broadman area [BA] 35 and 36), entorhinal cortex (ERC) and para hippocampal cortex (PHC) (Milner, 2005; Squire, 2009). It was subsequently discovered that surgical lesion in HM extended beyond hippocampus and included anterior para hippocampal gyrus and although isolated hippocampus damage causes significant memory impairments, they are not as severe as in the case of HM (Kirwan et al., 2008). Since neighbouring MTL structures both send and receive information to and from the hippocampus, understanding of the hippocampal function will not be complete without studying surrounding MTL structures (Manns & Eichenbaum, 2007; Rosene & Van Hoesen, 1987; Vago et al., 2014).

For instance, Rugg and Vilberg (2013) have proposed that hippocampus combines contextual information from PHC and object-related information from PRC. Functional specialisation also exist within the hippocampus itself (Small, 2014). Cornu Ammonis (CA) 3 and dentate gyrus (DG) are associated with encoding/early retrieval and CA1 was associated with consolidation/late retrieval (Mueller et al., 2011). Additionally, CA3 and DG regions were also proposed to play a role in pattern separation (Leutgeb et al., 2007). The subiculum (SUB) has been speculated to be associated with memory consolidation and memory recall (Ledergerber & Moser, 2017). However, these findings are in no way unequivocal and the understanding of memory organisation is far from complete (Travis et al., 2014). As Tulving (2002) stated, memory is a conglomerated system of more elementary operating components but identifying the specific operational role of each component and its neural correlate has been challenging.

AD patients represents a potential population for investigation of specific memory component subserved by each MTL subregion as during early stages of AD, AD pathology selectively affects MTL subregions (Braak & Braak, 1991). Pathologic tau-related neurofibrillary tangles (NFT) are the neuropathological hallmark of AD (Jack et al., 2018; McKhann et al., 1984) and closely correlates with regional brain atrophy (De Souza et al., 2012; Jack et al., 2018; Lindberg et al., 2017; Tardif et al., 2018; Whitwell et al., 2008), clinical symptoms, severity and progression of AD (Ingelsson et al., 2004). Additionally, during early stages of AD, NFT distribution also follows a stereotypical pattern appearing first in the BA 35 and in the ERC. Subsequently, NFTs can be found in hippocampal subfield CA1 before they spread further to neighbouring regions such as the subiculum (SUB) and then cortical regions outside the MTL (Braak & Braak, 1995; Braak & Del Tredici, 2020). Since pattern of brain atrophy closely tracks the pattern of NFT distribution (de Flores et al., 2020) and both NFT and atrophy influence phenotypic presentation (Jack et al., 2002; Murray et al., 2011; Whitwell et al., 2008), accurate characterisation of subregional atrophy measure seen on MRI can be used as a neuroimaging correlate of memory sub-functions. Additionally, predictable sequence of atrophy also allows for stage-based correlation with cognitive deterioration (Nelson et al., 2009).

However heterogeneity exists within AD and age at onset is one of the sources of heterogeneity (Tellechea et al., 2018). AD is commonly categorised into early onset AD (EOAD) and late onset AD (LOAD) based on the age at onset at 65 (Rossor et al., 2010). However, age is

not the only difference between the two forms of AD (Koedam et al., 2010) and clinical and neuropathological differences exist (Mendez, 2017). Clinically, LOAD tends to present predominantly with memory symptoms whereas a higher proportion of EOAD patients present with non-amnestic atypical symptoms (Mendez, 2012; Rossor et al., 2010). In keeping with this, higher neo-cortical involvement and relative sparing of hippocampus is more frequently found among EOAD (Ayodele et al., 2021). However, amnesia is still the most common presentation in EOAD (Ferreira et al., 2020; Harvey et al., 2003) but overlap in neural substrates underlying amnestic symptoms EOAD and LOAD remains an open question.

As atrophy pattern modulates presenting symptoms of AD (Murray et al., 2011; Whitwell et al., 2008), we hypothesise that both EOAD and LOAD of amnestic type will have similar MTL subregional atrophy. The aim of this study is to test this hypothesis. Although MTL atrophy has been well demonstrated in LOAD (de Flores, La Joie, & Chételat, 2015) MTL atrophy in AD patients with an earlier onset is less studied. To my knowledge, only one study attempted to map atrophy patterns in typical EOAD (Grinberg et al., 2020). Unlike LOAD, the relatively low prevalence combined with variant-related heterogeneity (Murray et al., 2011; Whitwell et al., 2008) adds to the complexity of establishing the typical atrophy pattern in EOAD. It is important to compare EOAD and LOAD using data obtained with the same image acquisition and processing methods as methodological differences, for instance, in segmentation protocols might make comparing findings across studies difficult (Wisse et al., 2014). Therefore, this study aims to compare the topography of MTL subregional atrophy in EOAD and LOAD of amnestic type to the typical well-established pattern of neurodegeneration in AD (Bobinski et al., 1997; Braak & Braak, 1991; West et al., 1994; Wolk et al., 2017).

Moreover, existing studies mostly focused on the hippocampus but research on extrahippocampal regions is rather scarce (Cavedo et al., 2014). For example, *in vivo* measurement of perirhinal cortex received little attention despite a part of this structure called BA35 being the site of earliest NFT formation (Braak & Braak, 1991). This is a critical omission, as extrahippocampal regions such as ERC and BA35 are also vulnerable to AD pathology and even precedes AD pathology in the hippocampal formation (Braak & Braak, 1991; Braak & Braak, 1995). Therefore, this study aims to investigate not only hippocampal atrophy but also the atrophy of the surrounding extrahippocampal regions in EOAD and LOAD. Our research interest

is to establish the topography of subregional atrophy pattern in the in EOAD and LOAD as a preliminary step towards correlating cognitive deficits with functional specialisation of MTL substructures.

There is partial evidence that the MTL region is invariably affected by AD pathology in both early and late onset groups. At autopsy, amnestic AD patients (majority of the sample were EOAD with mean age of symptoms onset = 60.8 years, *SD* = 10.5) had significant NFT pathology in SUB at least in advanced stages (Braak's stage VI) (Petersen et al., 2019). Moreover, comparable NFT density in CA1 and SUB in both EOAD and LOAD were found (Spina et al., 2021) and in both studies participants harboured sufficient NFT pathology to have Braak stage higher than III indicating that MTL regions were similarly affected in both EOAD and LOAD (Petersen et al., 2019; Spina et al., 2021). *In vivo* evidence converges with above-mentioned autopsy findings demonstrating that EOAD and LOAD had similar tau burden in the MTL regions captured by positron emission tomography (PET) (Schöll et al., 2017). Therefore, if perhaps EOAD and LOAD share similar NFT pathology, we speculate that both groups will display similar MTL subregional atrophy.

Comparison of atrophy in EOAD and LOAD has been challenging as hippocampal atrophy is associated not only with NFTs (Murray et al., 2011) but also with aging (de Flores, La Joie, et al., 2015a; Raji et al., 2009; Raz et al., 2005) as well as other non-AD-related neurodegenerative diseases (Maruszak & Thuret, 2014) which are more prevalent in older people (Spina et al., 2021). TAR DNA-binding protein 43 (TDP-43) deserves special attention as it often comorbid with AD (James et al., 2016; Nelson et al., 2019) and associated with hippocampal volume loss even in individuals with significant AD pathology (Josephs et al., 2017; Nelson et al., 2013). It was approximated that 25-59% of subjects with AD had concomitant TDP-43 (Amador-Ortiz et al., 2007; Josephs et al., 2015). TDP-43 co-pathology is also more prevalent in LOAD compared to EOAD (35% vs 8%) (Spina et al., 2021). It has been shown that TDP-43 tends to have a predilection for anterior hippocampus (aHPC) and NFT preferentially affects posterior hippocampus (pHPC) (de Flores et al., 2020). Therefore, differences due to the effects of ageing and increasing co-morbid pathologies might make atrophy patterns in EOAD and LOAD to diverge. In order to account for age-related variations, this study will compare EOAD

and LOAD to healthy controls of the corresponding age category. In order to infer the presence of TDP-43, we will also compare anterior hippocampal volumes in EOAD and LOAD.

An additional caveat concerning with studying AD in clinical population is that at the clinical stage, MTL atrophy had become widespread and focal atrophies might become less pronounced (Whitwell et al., 2007). Evidence suggests that there is a degree of convergence in atrophy pattern at advanced stages (Ossenkoppele et al., 2015). Therefore, at clinical stages, atrophy patterns will be less differentiated. For example, focal atrophy of the CA1 subfield was more prominent in the early (predementia or even preclinical) stages of AD, before atrophy becomes more widespread at the dementia stage, consistent with the pathological literature (de Flores, La Joie, & Chételat, 2015). We sympathise with the proposition by (Petersen et al., 2019) that if EOAD patients deviate from typical atrophy pattern, NFT accumulation must be absent in MTL regions known to get affected in early stages of AD pathology. We reason that if MTL subfield atrophy in EOAD and LOAD are different, differences will be most pronounced in early stages of AD and in earliest affected MTL subregions (for instance, BA35 and ERC).

To this end, studying amnestic mild cognitive impaired (aMCI) group might prove very informative. Mild cognitive impaired (MCI) patients exhibit significant cognitive impairments which deviate from normal healthy aging but are insufficient to meet an AD diagnosis (Maruszak & Thuret, 2014; Petersen et al., 1999). Several patients with MCI displayed atrophy pattern similar to AD (Shiino et al., 2008) and approximately 80% of aMCI converts to AD (Petersen, 2004). MCI and particularly the amnestic subtype (aMCI), is considered as a transitional stage between normal aging and a diagnosis of clinically probable AD (Whitwell et al., 2007). Therefore, in order to infer the atrophy pattern in EOAD and LOAD during earlier stages, we will compare MTL subfield atrophy in early onset MCI (EOMCI) and late onset MCI (LOMCI) groups to healthy controls of corresponding age group. We will only include MCI patients with positive AD pathology cross-validated by both cerebrospinal fluid (CSF) amyloid and tau positron emission tomography (tau-PET) measures.

Hypotheses

Braak et al. (2006) found that NFT accumulation at autopsy invariably followed a stereotypical pattern with initial appearance in the BA35 followed by limbic regions and eventually in the neocortex. In MRI, BA35 atrophy is detectable early in the course of the AD

even before the emergence of clinical symptoms followed by the atrophy in the ERC, PHC and the hippocampus as the disease progresses to clinical AD (Wolk et al., 2017; Xie et al., 2019). Similarly, using tau PET, Berron et al. (2021) found that tau was detectable in BA35 followed by the anterior and posterior hippocampus even in the early stages of MCI and at later MCI stage, BA36 and PHC were involved. Since this pattern is corroborated by multiple methodologies, we reason that this pattern reflects differential vulnerability of MTL subfields to AD pathology. Therefore, our hypotheses are made in reference to this stereotypical pattern of atrophy. Subfields hypothesised to show group differences are summarised in table 1 and 2.

Early onset MCI (EOMCI), Late onset MCI (LOMCI) and healthy control (HC)

PET scan showed that NFT deposition in BA35 and ERC preceded CA1 and SUB (Berron et al., 2021). Therefore, we reason that if MCI and AD exist on a continuum, we should also observe that both EOMCI and LOMCI groups have smaller BA35 and ERC compared with HC of corresponding age. Previous studies reported differences between healthy controls and aMCI patients in CA1 (Pluta et al., 2012), SUB (Hanseeuw et al., 2011) and both CA1 and SUB (La Joie et al., 2013). Therefore, we postulate that CA1 and SUB volumes in EOMCI and LOMCI will be smaller compared YHC and OHC. Following NFT deposition in CA1 and SUB, NFT spreads to BA36 and PHC in later MCI stage (Berron et al., 2021). Therefore, we also expect both EOMCI and LOMCI groups to show BA36 and PHC volume reduction as compared to healthy controls of their own age category.

If EOMCI is similar to EOAD and has a more rapid deterioration, EOMCI might show greater atrophy than LOMCI in subregions that are affected later in the NFT pathological cascade, namely, BA36 and PHC. Additionally, Spina et al. (2021) reported that tau pathology targeted posterior hippocampus (pHPC). Therefore, if AD pathology is more severe in EOMCI, pHPC is likely to be smaller in this group compared to LOMCI. DG is reported to be rather resistant to AD pathology in earlier stages (Ohm, 2007). Corroborating this, CA2-CA3-CA4-DG composite region showed no difference between MCI and healthy controls (de Flores, La Joie, & Chételat, 2015). Therefore, we do not expect DG deterioration at MCI stage and posit that there will be comparable DG subfield volume between EOMCI and YHC as well as between LOMCI and OHC. Due to age-related volume loss in CA1 and SUB (de Flores, La Joie, et al., 2015a), LOMCI might have smaller CA1 and SUB volumes than EOMCI. If LOMCI, much the same as

LOAD, also have higher prevalence of comorbid TDP-43 (Spina et al., 2021), anterior hippocampus (aHPC) volume in LOMCI might be smaller than that in EOMCI.

EOMCI vs YHC

Hypothesis 1a: EOMCI group will have significantly smaller BA35, ERC, BA36, PHC, CA1 and SUB as compared to YHC.

Hypothesis 1b: EOMCI will not be significantly different from YHC in DG volume.

LOMCI vs OHC

Hypothesis 2a: LOMCI group will have significantly smaller BA35, ERC, BA36, PHC, CA1 and SUB as compared to OHC.

Hypothesis 2b: LOMCI will not be significantly different form OHC in DG volume.

EOMCI vs LOMCI

Hypothesis 3a: There will be no significant group differences in the volumes of BA35, ERC and DG between EOMCI and LOMCI after controlling for sex and intracranial volume (ICV).

Hypothesis 3b: EOMCI will have significantly bigger CA1, SUB and aHPC than LOMCI after controlling for sex and ICV.

Hypothesis 3c: EOMCI will have significantly smaller BA36, PHC and pHPC than LOMCI after controlling for sex and ICV.

Table 1

Summary of hypotheses for comparison of MCI and HC (" < " indicates that the former group will have bigger volume in the subfields listed as compared with the latter group)

	Group comparison			
	YHC > EOMCI	OHC > LOMCI	EOMCI > LOMCI	LOMCI > EOMCI
MTL Subregions	BA35, ERC, CA1 SUB, PHC, BA 36	BA35, ERC, CA1 SUB, PHC, BA 36	CA1, SUB, aHPC	BA36 PHC pHPC

Young healthy control vs EOAD

Since young healthy controls (YHC) might have relatively fewer co-pathology and age-related neuroanatomical changes (de Flores, La Joie, & Chételat, 2015; Spina et al., 2021), we postulate that we will observe a stark contrast in all MTL subregional volumes between EOAD and YHC.

Hypothesis 4: All subregions of MTL: BA35, BA36, ERC, PHC, CA1, SUB and DG in EOAD will be significantly smaller compared to YHC.

Old healthy control vs LOAD

A previous study found that in healthy aging, age-related atrophy was significant only in CA1 and SUB (de Flores, La Joie, et al., 2015a). Therefore, the differences in CA1 and SUB between old healthy controls (OHC) and LOAD might be less pronounced due to age-related volume loss (de Flores, La Joie, et al., 2015a). Differences might still be detectable given that AD-related neuronal loss (Bobinski et al., 1997; West et al., 1994) is several magnitudes greater than age-related neuronal loss (de Flores, La Joie, & Chételat, 2015) for AD-related atrophy to be completely masked by age-related atrophy. Therefore, we expect that all MTL subfield volumes in LOAD will be smaller than those in OHC.

Hypothesis 5: All subregions of MTL: BA35, ERC, BA36, PHC, CA1, SUB and DG in LOAD will be significantly smaller than those in OHC.

EOAD vs LOAD

In light of partial evidence that both EOAD and LOAD harboured NFT pathology in MTL (Petersen et al., 2019; Spina et al., 2021) and since our sample is limited to typical amnestic form, we hypothesise that EOAD and LOAD would have comparable MTL tau pathology. Due to age-related volume loss in CA1 and SUB (de Flores, La Joie, et al., 2015a), LOAD might have smaller CA1 and SUB than EOAD. Since EOAD has been reported to take a more aggressive course (Bateman et al., 2011; Holland et al., 2012; Tellechea et al., 2018; van der Flier et al., 2011), we expect that EOAD will show more severe involvement of BA36, PHC as these regions are reported to get affected later in the disease progress (Berron et al., 2021). Additionally, since DG is relatively resistant to AD until later stages (Ohm, 2007; Small et al., 2002; West et al., 1994) and EOAD deteriorates more severely (Bateman et al., 2011; Holland et al., 2012; Tellechea et al., 2018; van der Flier et al., 2011), we hypothesise that EOAD might have smaller DG than LOAD. Additionally, as it is likely that TDP-43 preferentially targets aHPC (de Flores et al., 2020) and given the higher prevalence of TDP-43 in older individuals (de Flores et al., 2020; Spina et al., 2021), we also expect to observe smaller aHPC volume in LOAD. As mentioned above, if AD pathology is more advanced in EOAD (Bateman et al., 2011; Holland et al., 2012; Tellechea et al., 2018; van der Flier et al., 2011), pHPC which is targeted by tau pathology (Spina et al., 2021) is likely to be smaller in EOAD as compared with LOAD.

Hypothesis 6a: There will be no significant group differences in the volumes of BA35 and ERC, between EOAD and LOAD after controlling for sex and intracranial volume (ICV).

Hypothesis 6b: EOAD will have significantly bigger CA1 and SUB compared to LOAD after controlling for sex and ICV.

Hypothesis 6c: EOAD will have significantly smaller volumes in BA36, PHC, DG and pHPC compared to LOAD after controlling for sex and ICV.

Hypothesis 6d: LOAD will have significantly smaller aHPC than EOAD after controlling for sex and ICV.

Table 2

Summary of hypotheses for comparison of AD and HC (“ < ” indicates that the former group will have bigger volume in the subfields listed as compared with the latter group)

	Group comparison			
	YHC > EOAD	OHC > LOAD	EOAD > LOAD	LOAD> EOAD
MTL Subregions	BA35, ERC, CA1 SUB, PHC, BA36, DG	BA35, ERC, CA1 SUB, PHC, BA36 DG	CA1, SUB, aHPC	BA 35 PHC DG pHPC

Ethical approval

The data come from Swedish Biofinder2 study. The Regional Ethics Committee in Lund, Sweden, has approved the study design and the consent in 2016 (reference 1053). All patients have given their written informed consent and all data are analysed without access to personal information. Approval for PET imaging was obtained from the Swedish Medical Products Agency.

Method

Participants

Healthy controls

Controls are neurologically and cognitively healthy individuals. The inclusion criteria are: i) age 43-65 years (young control) and age 71-100 years (old control); ii) absence of cognitive symptoms as assessed by a physician specialised in cognitive disorders; iii) Mini-Mental State Examination (MMSE) (Folstein et al., 1975) score 27-30 (young control) or 26-30 (old control) at screening visit; iv) do not fulfil the criteria for mild or major neurocognitive disorder (MCI or

dementia) according to DSM-5 (American Psychiatric Association, 2013); and v) fluent in Swedish.

MCI sample

Inclusion criteria for MCI are: i) ages 40-100 years; ii) referred to the memory clinics due to cognitive symptoms; iii) MMSE score of 24-30 points; iv) does not fulfill the criteria for any dementia (major neurocognitive disorder) according to DSM-5 (American Psychiatric Association, 2013) v) fluent in Swedish. Biomarker evidence of both amyloid beta (Aβ) (validated using CSF Aβ) and pathologic tau (validated using tau-PET) must be present. In order to form an amnestic MCI group (aMCI), we picked MCI patients with memory scores 1.5 SD lower than the norm in cognitively unimpaired controls of their own age category. Memory test will be described in detail below under "cognitive tests" section. The aMCI group was subdivided into early onset amnestic MCI (EOMCI) and late onset amnestic MCI (LOMCI) with the age cut-off of EOMCI ≤ 65 years and LOMCI > 70 years. Since atrophy precedes symptoms in AD, we set a more liberal age cut-off at 70 to avoid including early onset cases to late onset group.

AD sample

Clinical diagnosis was made by a physician based on clinical criteria in DSM-5 (American Psychiatric Association, 2013) without the support of biomarkers. To limit our AD sample to typical variant as much as possible, we will include individuals with memory score 1.5 SD below the mean score of healthy controls of their age category with no cognitive impairment. Memory test will be described in detail below under "cognitive tests" section. EOAD group consists of AD patients who are ≤ 65 years and LOAD group consists of AD patients > 70 years.

MRI acquisition

Structural MRI was performed using a Siemens 3T MAGNETOM Prisma scanner (Siemens Medical Solutions), with high resolution T1-weighted (1x1x1 mm3) and T2-weighted (0.4 × 0.4 × 2.0 mm3) anatomical magnetization-prepared rapid gradient echo (MPRAGE) images. Automatic Segmentation of Hippocampal Subfields [ASHS-T1]) for the segmentation of MTL subregions, including anterior/posterior hippocampus, entorhinal cortex (ERC), Brodmann areas (BA) 35 and 36, and PHC on T1w MRI (Xie et al., 2019). Estimate of intracranial volume (ICV), median thickness of MTL subregions including anterior hippocampus, BA 35 and BA36,

ERC and PHC were obtained from T1-weighted images. Hippocampal subfield volumes: CA1, DG and subiculum (SUB) was obtained from high-resolution T2-MRIs using the Automated Segmentation for Hippocampal Subfields (ASHS-T2) software (Yushkevich et al., 2015), with a manual protocol as described in Berron et al. (2017). All MRI scans and subfield labels were visually inspected for quality, and the segmentations were edited when necessary. In some participants, a subset of MTL regions did not have sufficient quality to be included in the analyses. As a result, the number of subjects for a given MTL measure varies. All volume and thickness of subfield measures were average of the left and right values.

CSF Aβ42, CSF Aβ40

At Eli Lilly and Company, analysis of CSF Aβ42 and CSF Aβ40 using Meso Scale Discovery immunoassays (MSD; Rockville, MD, USA). In BioFINDER-2, Aβ PET is by design performed only cognitively normal individuals and those with MCI and thus CSF Aβ42/Aβ40 was chosen to ensure a common measure of Aβ pathology across all participants.

Aβ-status (positive/negative) was defined using CSF Aβ42/Aβ40 with a cut-off of <0.752 (determined using Gaussian mixture modelling) (Bertens et al., 2017).

[18F]RO948 Tau-PET

Tau PET with dynamic (list-mode) studies was performed using [^{18}F]RO948 (Kuwabara et al., 2018), on digital GE Discovery MI scanners over 70-90 min post injection of ~370 MBq [18F]RO948. Standardized uptake value ratio (SUVR) were created using the inferior cerebellar cortex as reference region (Baker et al., 2017). A high- resolution T1-weighted MRI was used for PET image co-registration and template normalization. Volume weighted FreeSurfer-based (FreeSurfer v6.0 (https://surfer.nmr.mgh.harvard.edu/) composite regions of interest (ROI) for tau-PET were created based on volume-weighted average (of left and right) scores of ERC, inferior temporal cortex, medial temporal cortex, fusiform gyrus, parahippocampal cortex and amygdala (Leuzy et al., 2020). This ROI encompasses brain regions affected in Braak and Braak's stages I-IV (Braak & Braak, 1995). Tau positivity was determined based on the predefined cut-off of mean plus 2.5 SDs (Br I-IV ROI > 1.36 SUVR) in Aβ-negative young controls (Leuzy et al., 2020).

Cognitive tests

As a test for memory, participants were administered the delayed 10-word-list-recall test (ADAS delayed) from Alzheimer's Disease (AD) Assessment Scale-Cognitive Subscale (ADAS-Cog) (Rosen et al., 1984). The learning trial of the 10 words was repeated three times. After a distraction task (Boston Naming Test – 15 items short version), the participant freely recalled the 10 words ("delayed recall"). The performance was measured on a scale of 0-10 and delayed recall was scored as number of errors (i.e., 10 - correctly recalled words) such that a higher score meant worse memory performance. Means and standard deviations were established in cognitively unimpaired healthy controls and adjusted for age and education. The ADAS cut-off scores were ≥ 4 for 70 years and below ≥ 5 for more than 70 years old. Additionally, MMSE (Folstein et al., 1975) was administered to all participants.

Statistical analyses

Group comparisons

To analyse the effect of diagnostic group (EOAD, LOAD, EOMCI, LOMCI, YHC, OHC) on MTL subfields: extrahippocampal subfield volumes (BA35, ERC, PHC, BA36) and hippocampal subfield volumes (CA1, SUB, DG, aHPC, pHPC), linear models will be fitted with diagnostic group as independent (factor) variable, extrahippocampal and MTL subfield volumes as dependent variable and intracranial volume (ICV) and sex will be entered as covariates. ANCOVA with type III sum of squares will be fitted to the linear models to investigate whether diagnostic group has a significant effect on the means of the dependent variables adjusted for covariates. Pairwise group comparisons are considered significant if $p < 0.05$. To make the comparisons more meaningful, adjusted mean of each subfield volume in patient groups were expressed as percentage difference of the adjusted mean volume of respective subfield in healthy controls. Visual inspections were done to ensure all regression models meet assumption of multicollinearity, normality of error terms, linearity, homogeneity of variance and where applicable, homogeneity of slopes unless otherwise reported.

Exploratory analyses

Age effect on subfield volume

To investigate the effect of age on each MTL subfield volume in AD group as a whole, regressions models were fitted with age as an independent variable and each subfield as a dependent variable controlled for sex and ICV. The same analyses were repeated for MCI group as a whole to investigate the effect of age on each MTL subfield. We applied *t*-statistics for the linear regression coefficient and only *p* values < .050 were considered significant.

MTL-tau load (MTL tau-SUVr) and subfield volume

Additionally, to investigate the relationship between the amount of tau (tau burden) and MTL subfield volume, we also conducted Pearson's correlations between MTL tau PET signal (tau-SUVr) values and each MTL subfield volume.

Cognitive scores

Pearson's correlation analyses were performed to assess the relationship between each MTL subfield volume and ADAS and MMSE scores in AD group. MTL tau-SUVr were also correlated with MMSE and ADAS scores in AD group.

Pearson's correlation analyses were performed to assess the relationship between each MTL subfield volume and ADAS and MMSE scores in MCI group. MTL tau-SUVr were also correlated with MMSE and ADAS scores in MCI group.

All analyses were performed in R v3.3.2 (www.r-project.org).

RESULTS

Descriptive statistics

Descriptive characteristics of the samples: age, sex ratio, education, cognitive scores are summarised in the table below.

Table 3

Demographic data

	EOAD	LOAD	EOAD > LOAD	EOMCI	LOMCI	EOMCI > LOMCI	YHC	OHC	YHC > OHC
Age	61 (5)	77 (4)	NA	59 (4)	76 (3)	NA	54 (6)	75 (5)	NA
Sex (% of female)	69%	51%	NA	15%	47%	NA	57%	51%	NA
Total (*N*)	16	74	NA	6	32	NA	152	136	NA
Education (*Mean*, *SD*)	14 (3)	11 (4)	***p* < .050**	16 (4)	13 (5)	*p* > .050	14 (3)	12 (3)	***p* < .001**
MMSE (*Mean*, *SD*)	21 (4)	20 (4)	*p* >.050	28 (1)	26 (2)	***p* < .050**	29 (1)	29 (1)	*p*>.050
ADAS (*Mean*, *SD*)	8 (2)	9 (1)	***p* < .050**	9 (1)	7 (2)	***p* <.050**	2 (1)	3 (2)	***p* < .001**

Group comparisons

YHC vs EOMCI

EOMCI group had significant volume reductions in all MTL subfields (BA35, BA36, ERC, PHC, CA1 and SUB) except DG as compared with YHC after controlling for ICV and sex. The result of group comparison between YHC and EOMCI is summarised in table 4.

Table 4

Volume reduction in each MTL subfield volume in EOMCI compared to YHC (the subfields that showed significant reductions are in bold)

Group comparison	Subfield	% reduction	df	t-statistic	p-value
EOMCI < YHC	**BA35**	13.846	154	4.106	**<.001**
	BA36	9. 462	154	2.040	**<.050**
	ERC	8.134	154	2.408	**<.050**
	PHC	6.104	154	2.316	**<.050**
	CA1	22.107	134	2.563	**<.050**
	SUB	17.195	154	3.481	**<.001**
	DG	2.291	135	0.347	>.050

Figure 1

Percentage of volume loss in YHC compared to EOMCI in BA35, BA36, ERC, PHC, CA1, SUB and DG

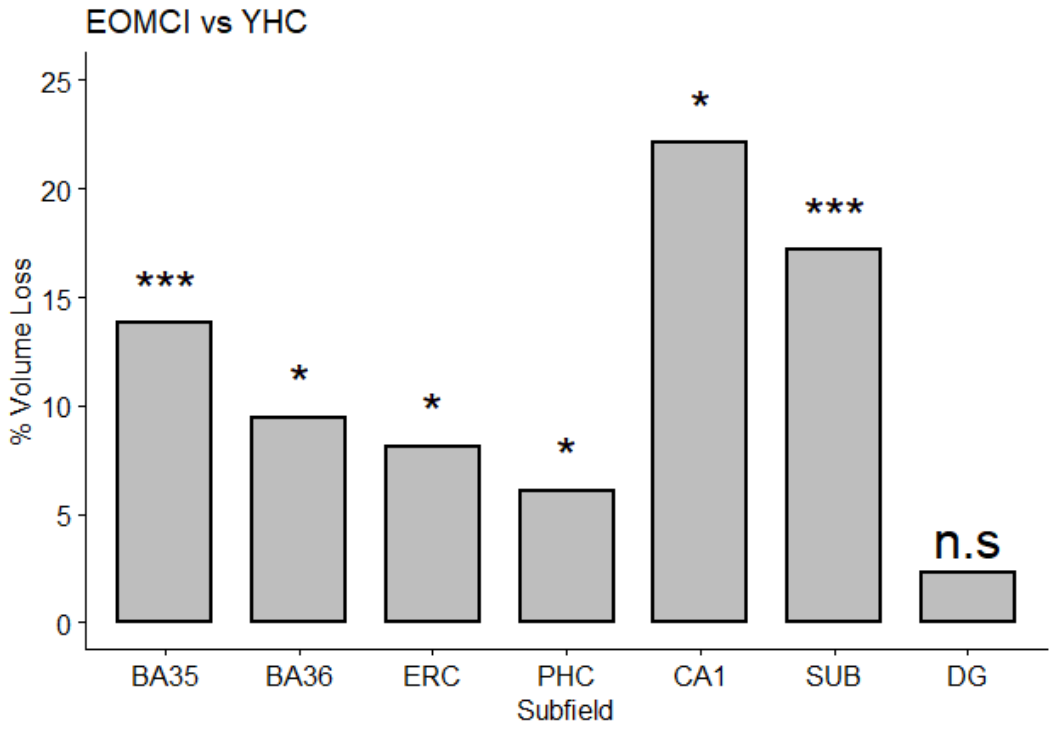

(Significance codes: 0.001 '***' 0.01 '**' 0.05 '*' n.s 'not significant')

OHC vs LOMCI

LOMCI group had significant volume reduction in all MTL subfields (BA35, BA36, ERC, PHC, CA1, SUB and DG) as compared with OHC after controlling for ICV and sex. The result of group comparison between OHC and LOMCI is summarised in table 5.

Table 5

Volume reduction in each MTL subfield volume in LOMCI compared to OHC

Group comparison	Subfield	% reduction	df	t-statistic	p-value
LOMCI < OHC	**BA35**	7.643	173	4.669	**<.001**
	BA36	3.880	173	2.309	**<.050**
	ERC	7.075	173	5.088	**<.001**
	PHC	3.022	173	2.339	**<.050**
	CA1	11.500	149	3.468	**<.001**
	SUB	15.251	175	6.223	**<.001**
	DG	8.109	149	2.671	**<.010**

Figure 2

Percentage of volume loss in OHC compared to LOMCI in BA35, BA36, ERC, PHC, CA1, SUB and DG

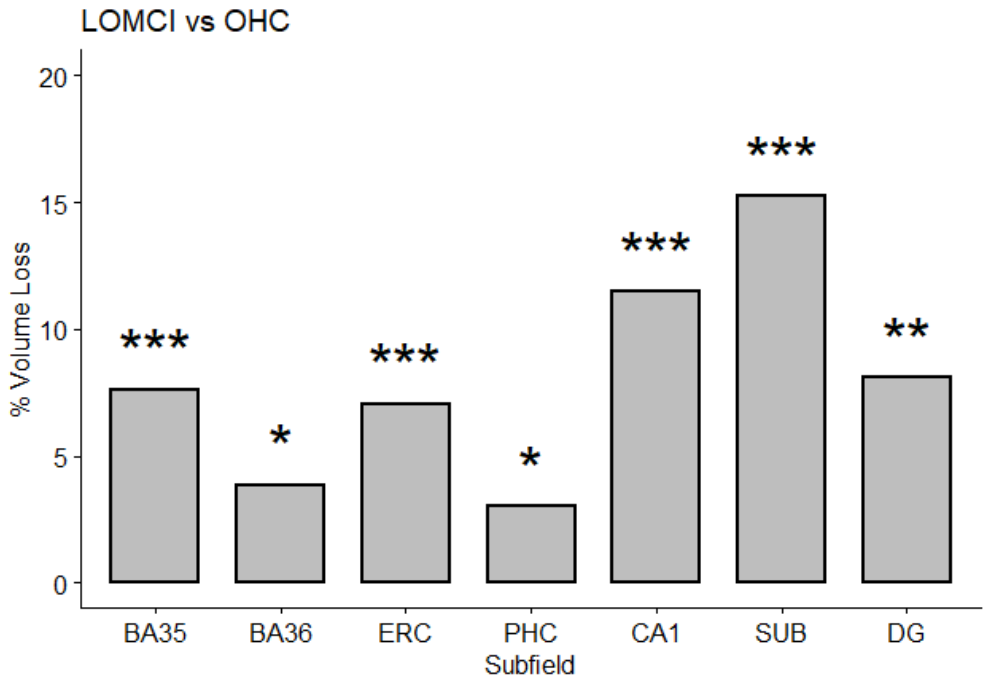

(Significance codes: 0.001 '***' 0.01 '**' 0.05 '*' n.s 'not significant')

EOMCI vs LOMCI

None of the MTL subfields (BA35, BA36, ERC, PHC, CA1, SUB, DG, aHPC and pHPC) showed significant volume difference when LOMCI group and EOMCI were compared controlling for ICV and sex. The results of group comparison between EOMCI and LOMCI is summarised in table 6 and 7.

Table 6

MTL subfield volume reduction in LOMCI compared to EOMCI (note LOMCI < EOMCI)

Group comparison	Subfield	% difference	df	t-statistic	p-value
LOMCI < EOMCI	ERC	0.847	34	-0.199	>.050
	PHC	1.954	34	-0.555	>.050
	CA1	2.311	24	-0.205	>.050
	SUB	5.103	34	-0.704	>.050
	DG	10.791	24	-1.139	>.050
	aHPC	6.421	32	-0.831	>.050

Table 7

MTL subfield volume reduction in EOMCI compared to LOMCI (note EOMCI < EOMCI)

Group comparison	Subfield	% difference	df	t-statistic	p-value
EOMCI < LOMCI	BA35	-1.070	34	0.250	>.050
	BA36	-1.073	34	0.237	>.050
	pHPC	-2.947	32	0.405	>.050

YHC vs EOAD

EOAD group had significant volume reduction in all MTL subfields (BA35, BA36, PHC, CA1, SUB and DG) as compared with YHC after controlling for ICV and sex except for ERC. The results of group comparison between YHC and EOAD is summarised in table 8.

Table 8

Volume reduction in each MTL subfield volume in EOAD compared to YHC (the subfields that showed significant reductions are in bold)

Group comparison	Subfield	% reduction	df	t-statistic	p-value
EOAD < YHC	**BA35**	10.113	163	4.941	**<.001**
	BA36	5.691	163	2.070	**<.050**
	ERC	3.116	163	1.452	>.050
	PHC	6.040	163	3.554	**<.001**
	CA1	14.201	146	3.782	**<.001**
	SUB	15.682	164	5.881	**<.001**
	DG	11.553	146	3.450	**<.001**

Figure 3

Percentage of volume loss in EOAD compared to YHC in BA35, BA36, ERC, PHC, CA1, SUB and DG

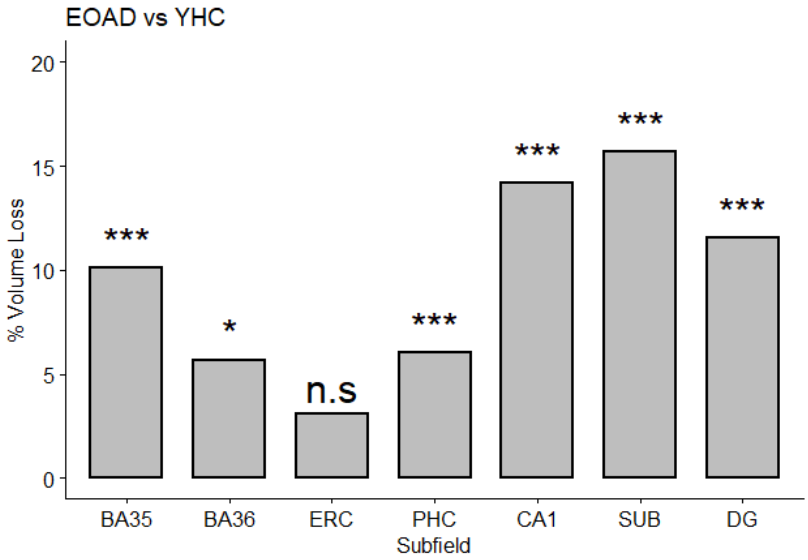

(Significance codes: 0.001 '***' 0.01 '**' 0.05 '*' n.s 'not significant')

OHC vs LOAD

LOAD group had significant volume reduction in all MTL subfields (BA35, BA36, ERC, PHC, CA1, SUB and DG) as compared with OHC after controlling for ICV and sex. The results of group comparison between OHC and LOAD is summarised in table 9.

Table 9

Volume reduction in each MTL subfield volume in LOAD compared to OHC (the subfields that showed significant reductions are in bold)

Group comparison	Subfield	% reduction	df	t-statistic	p-value
LOAD < OHC	**BA35**	11.580	177	7.556	**<.001**
	BA36	7.671	177	5.335	**<.001**
	ERC	12.357	177	9.306	**<.001**
	PHC	9.353	177	8.175	**<.001**
	CA1	19.014	149	7.847	**<.001**
	SUB	18.363	178	11.117	**< .001**
	DG	13.315	148	5.877	**<.001**

Figure 4

Percentage of volume loss in LOAD compared to OHC in BA35, BA36, ERC, PHC, CA1, SUB and DG

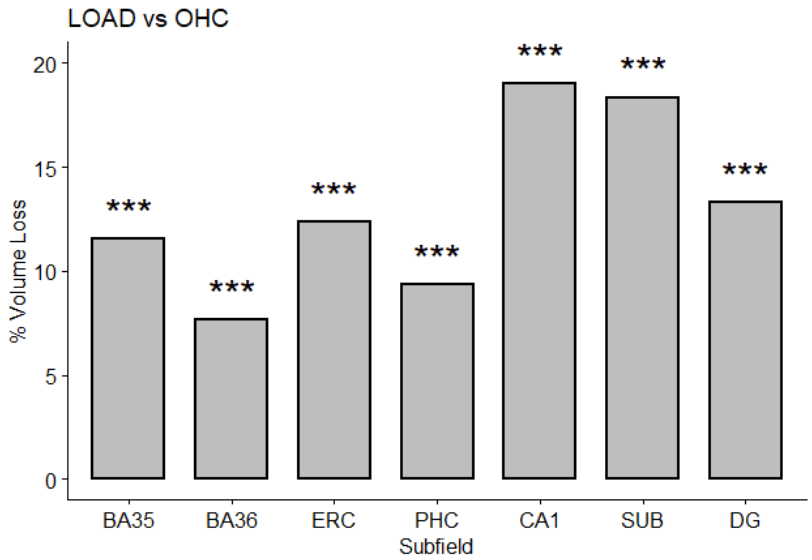

(Significance codes: 0.001 '***' 0.01 '**' 0.05 '*' n.s 'not significant')

EOAD vs LOAD

BA35 and BA36 and DG volumes were comparable between EOAD and LOAD group. EOAD group had significantly smaller ERC, PHC, CA1, SUB as compared with LOAD after controlling for ICV and sex. EOAD group had significantly bigger aHPC and pHPC than LOAD

after controlling for ICV and sex. The results of group comparison between EOAD and LOAD is summarised in table 10.

Table 10

Volume reduction in each MTL subfield volume in LOAD compared to EOAD (the subfields that showed significant reductions are in bold)

Group comparison	Subfield	% difference	df	t-statistic	p-value
LOAD vs EOAD	BA35	5.695	85	-1.650	>.050
	BA36	4.708	85	-1.470	>.050
	ERC	7.886	85	-2.391	**<.050**
	PHC	8.263	85	-3.480	**<.001**
	CA1	11.971	67	2.500	**<.050**
	SUB	11.382	86	-3.063	**<.010**
	DG	5.913	67	-1.632	>.050
	aHPC	13.608	76	-2.503	**<.050**
	pHPC	15.234	76	-3.254	**<.010**

Figure 5

Percentage of volume loss in LOAD compared to EOAD in pHPC, aHPC, BA35, BA36, ERC, PHC, CA1, SUB and DG

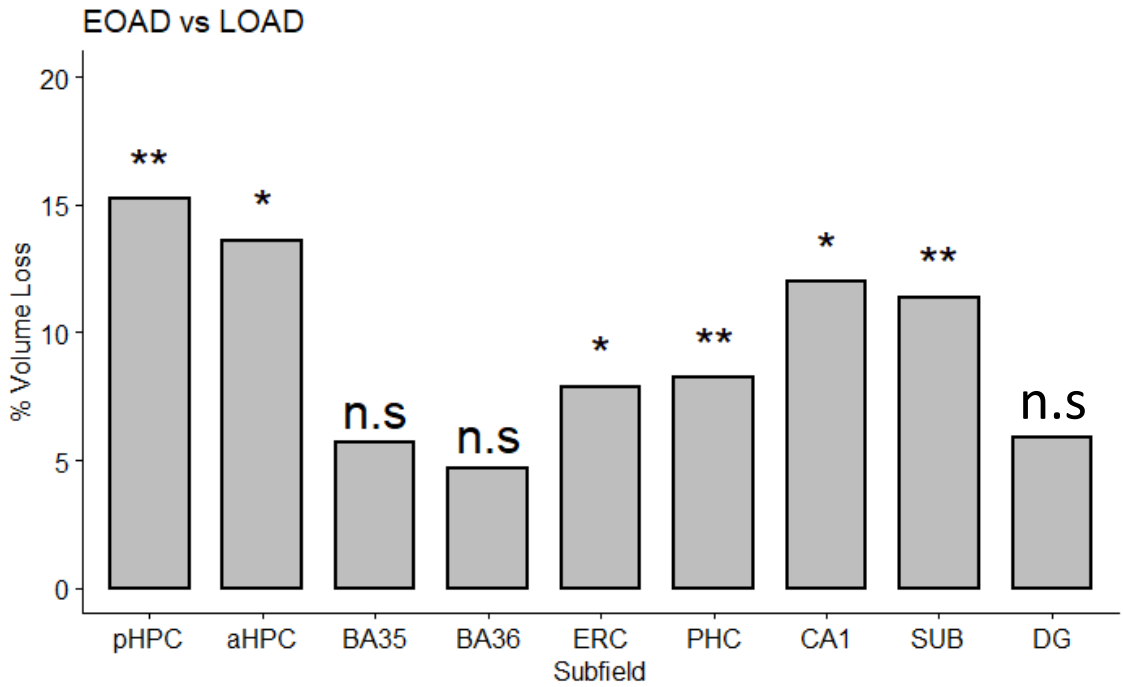

(Significance codes: 0.001 '***' 0.01 '**' 0.05 '*')

Relationship among MTL-tau, MTL subfield volumes and cognitive scores in MCI

There is no significant correlation between MTL-tau and all MTL subregion volume in MCI group.

MTL-tau has a marginally significant correlation with ADAS ($r(47) = 0.284$, $p < .050$) but not with MMSE scores. No correlation between each MTL subfield volume and MMSE score. No correlation between each MTL subfield volume and ADAS score.

Relationship among MTL-tau, MTL subfield volumes and cognitive scores in AD

MTL-tau is associated with BA36 volume ($r(103) = -0.300$, $p < .010$) but with no other subfield. MTL-tau does not correlate with ADAS score but correlated with MMSE score ($r(104) = -0.225$, $p < .050$).

All MTL subfield volumes are significantly correlated with ADAS scores: BA35 volume ($r(103) = -0.369$, $p < .001$), BA36 volume ($r(103) = - .008$, $p < .050$), ERC volume ($r(103) = -0.487$, $p < .001$), PHC volume ($r(83) = -0.360$, $p < .001$), CA1 volume ($r(104) = -0.472$, $p < .010$), SUB volume ($r(83) = -0.358$, $p < .050$), DG volume ($r(83) = 0.295$, $p < .010$).

BA 36 is significantly correlated with MMSE score ($r(103) = 0.243$, $p < .050$) no other region has correlation with MMSE score.

Effect of age on subfield volume in AD

Age is predictive of PHC, CA1, SUB and DG volume after controlling for sex and ICV in AD group as a whole.

Table 11

Coefficient table of age as a predictor of each MTL subfield covaried for sex and ICV in AD group as a whole (EOAD+LOAD). Age has negative effect on subfields shown in bold.

Subfield	βcoefficient of age	df	t-statistic	p value
BA35	-3.130e-03	101	-0.904	>.050
BA36	-2.001e-03	101	-0.543	>.050
ERC	-4.030e-03	101	-1.301	>.050
PHC	-6.476e-03	101	-2.627	**<.010**
CA1	-2.597e+00	81	-2.023	**<.050**
SUB	-5.120e+00	102	-3.036	**<.010**
DG	-2.214e+00	81	-2.243	**<.050**

Effect of age on subfield volume in MCI

Age is predictive of ERC, PHC and SUB after controlling for sex and ICV in MCI group as a whole. Although we observed that age has a negative effect on ERC, PHC and SUB volumes in MCI group as a whole.

Table 12

Coefficient table of age as a predictor of each MTL subfield covaried for sex and ICV in MCI group as a whole (EOMCI+LOMCI). Age has negative effect on subfields shown in bold.

Subfield	β coefficient for age variable	df	t-statistic	P value
BA35	-6.366e-03	45	-1.736	>.050
BA36	-7.202e-03	45	-1.603	>.050
ERC	-7.948e-03	45	-2.263	**<.050**
PHC	-7.085e-03	45	-2.351	**<.050**
CA1	-3.452e+00	31	-1.469	>.050
SUB	-6.359e+00	45	-2.148	**<.050**
DG	-2.713e+00	31	-1.435	>.050

Discussion

The purpose of this study is to investigate whether the MTL subregional atrophy in EOAD and LOAD of the amnestic variant follows a similar pattern. To this end, we performed group comparisons between patient groups (EOAD, LOAD, EOMCI, LOMCI) and cognitively healthy controls of their own age category as well as direct comparison between patient groups. Generally, the findings of our study are in support of our main hypotheses. All patient groups reliably showed volume loss in various MTL subfields compared to healthy controls of their own age category. We found that the topography of MTL subregional atrophy in EOAD, LOAD, EOMCI and LOMCI resemble the topography of regional NFT distribution of Braak and Braak (1991). All patient groups generally displayed atrophy in BA35, ERC as well as in the hippocampus. In both MCI and AD groups, percentage of volume loss in different MTL subfields differed widely which corroborates that NFT pathology does not affect all MTL subregions uniformly (Braak & Braak, 1991).

MCI

We followed the reasoning by Petersen et al. (2019) that if EOAD differs from LOAD in the anatomical distribution of AD pathology, such differences will be most apparent in MTL subregions affected early in the disease process. Our study found that BA35, BA 36, ERC and PHC showed comparable atrophy in both EOMCI and LOMCI groups corroborating the highly replicated Braak and Braak (1991)-like pattern. This finding broadly matches pervious findings in

prodromal and preclinical stages of typical AD (Wolk et al., 2017; Xie et al., 2019). In Xie et al. (2019), atrophy was modest but detectable in BA35, BA36 and Wolk et al. (2017) also reported that BA35 and PHC showed volume decrease in early preclinical AD.

We postulated that if perhaps disease progression is more aggressive in EOMCI than LOMCI, EMOCI will show greater atrophy in BA 36 and PHC that were shown to be affected later MCI stage (Berron et al., 2021). However, EOMCI and LOMCI did not differ in BA36 and PHC volumes therefore EOMCI group in our study did not appear to be in a more advanced disease stage than LOMCI. MMSE score in EOMCI was also higher compared to LOMCI. Age has a significant negative effect on ERC, PHC and SUB and aHPC but age-related atrophy was not large enough to make significant group differences between EOMCI and LOMCI. Both aHPC and pHPC volumes are similar between EOMCI and LOMCI. Therefore, we can speculate that despite more advanced age, LOMCI sample in this study did not appear to have higher TDP-43 pathology.

Hippocampal atrophy was reported in preclinical stages of AD (Wolk et al., 2017; Xie et al., 2019). In line with previous finding in aMCI sample that showed significant volume loss in CA1 and SUB (de Flores, La Joie, et al., 2015b; La Joie et al., 2013), we also found that CA1 and SUB showed greatest amount of atrophy in both EOMCI and LOMCI compared to healthy controls. We postulated that due to age-related atrophy in LOMCI atrophy of CA1 and SUB in LOMCI will be greater than EOMCI but this was not supported by the results. It is worthy of note that EOMCI group was small and additionally, it only had one female thus controlling for gender might not have had any effect. Future studies should compare EOMCI and LOMCI in samples with similar proportion of both sexes.

Given previous findings that DG is relatively resilient (Ohm, 2007), we did not expect volume loss in DG at MCI stage. Our hypothesis found partial support. EOMCI did not show DG volume loss compared to healthy controls but LOMCI group had smaller DG compared to healthy controls. The findings on DG involvement at MCI stage is mixed. DG atrophy was present in prodromal AD (Wolk et al., 2017) and in amnestic MCI (Yushkevich et al., 2015). In contrary, de Flores, La Joie, et al. (2015b) and La Joie et al. (2013) only found significant atrophy in CA1 and SUB in MCI. However, in these two studies, DG was not evaluated separately but amalgamated into a composite volume (CA2/3/4/DG) thus possibly obscuring subtle changes in

DG. Interestingly, Pluta et al. (2012) found that in aMCI patients, ASHS-generated DG volumes were significantly different from controls but the differences disappeared after manual correction (Pluta et al., 2012). It can be interpreted that DG atrophy, if present, is subtle at MCI stage and might not be detectable by crude composite measures. This highlights the importance of methodological consistency among studies for meaningful comparison of findings. Another explanation for difference in DG volume between LOMCI and healthy controls could be due to the fact that AD negativity in healthy controls as well as AD positivity in MCI groups was confirmed by biomarker evidence. This ensured that healthy control group did not contain individuals with AD pathology and might have made the subtle contrast between LOMCI and healthy controls unobscured.

AD

As we hypothesised, in comparison to their healthy counterparts, EOAD group and LOAD group had significant volume reductions in all hippocampal and extrahippocampal regions involved in Braak and Braak (1991) staging except preservation of ERC in EOAD which was unexpected. As predicted, LOAD group showed smaller CA1 and SUB than EOAD which is in line with the findings that amnestic EOAD patients showed greater hippocampal atrophy (Mendez, 2012) and greater grey matter loss in MTL relative to age-matched healthy controls (Möller et al., 2013). Age is predictive of CA1 and SUB volume in our AD sample and the relationship is negative. Moreover, the prevalence of non-AD copathologies also increase with age (Spina et al., 2021). Therefore, age differences most likely explain smaller CA1 and SUB in LOAD compared to EOAD.

Finding that CA1 decreases in size with age is fairly unequivocal (Frisoni et al., 2005; Wisse et al., 2014) but findings regarding the association between aging and SUB is more variable. Subiculum atrophy has been reported as unrelated to aging but associated with AD-related pathology (Daugherty et al., 2016). But elsewhere, SUB is reported to have reduced volume in ageing (Chételat et al., 2008; La Joie et al., 2010) and even as one of the subfields most affected by ageing (Malykhin et al., 2017). Discrepancies could stem from different age range of the samples. Finding in our study suggests that SUB atrophy is associated with both aging and AD pathology.

Lastly, we hypothesised that BA36, PHC and DG would be more atrophied in EOAD compared to LOAD given the reports that EOAD tends to take more aggressive course (Bateman et al., 2011; Holland et al., 2012; Tellechea et al., 2018; van der Flier et al., 2011). However, we found that BA36 and DG volumes between EOAD and LOAD was comparable and PHC volume was smaller in LOAD than in EOAD. Given that LOAD group had smaller pHPC which is targeted by tau pathology (Spina et al., 2021), we can speculate that LOAD might in fact be in more advanced stage of AD. Since aPHC is smaller in LOAD than EOAD, we can also speculate that TDP-pathology might be higher in LOAD group. Furthermore, ERC volume loss was reported to be associated with TDP-43 pathology (de Flores et al., 2020) and LOAD sample in our study had smaller ERC volume compared to EOAD but ERC volume was preserved in our EOAD sample.

Cognitive scores

We also explored the relationship between MTL tau burden (MTL tau-PET SUVr), subfield atrophy and memory performance (ADAS score). In MCI group, ADAS score correlated with tau burden of MTL subfields (captured by composite MTL tau-PET SUVr) but not with MTL subfield volume. This is not surprising as synaptic loss takes place in terminal zones of neurons that are prone to develop tau tangles (Davies & Terry, 1981). Tau-related neurodegeneration (Ferreira et al., 2020) and synaptic loss (Ohm, 2007), even in the absence of overt brain atrophy might be sufficient to bring about memory symptoms (Ferreira et al., 2020; Ohm, 2007). This might explain the significant correlation between MTL tau burden and memory scores and the absence of correlation between MTL volume and memory scores in MCI group. This finding corroborates the previous finding that tau burden in MTL regions but not atrophy was associated with lower memory performance in cognitively unimpaired individuals and MCI patients (Berron et al., 2021).

In contrast, tau burden in AD had no relationship with ADAS scores and instead, subregional volumetry correlated with ADAS scores. It has been reported that in AD, cognitive decline correlates most closely with neuronal loss followed by tau burden (Petersen et al., 2019). This is consistent with the notion that AD biomarkers turn abnormal in a sequence starting with amyloid measures followed by tau measures, then structural MRI and subsequently by clinical symptoms (Jack & Holtzman, 2013). Although this is true for AD population, correlation

between ADAS score and tau burden in MCI stage might suggest that structural changes might not precede clinical symptoms. Given more general nature of ADAS delayed memory measure, our ability to infer specific function of each MTL subregions in this study is limited.

Nonetheless, we infer that MTL tau burden would be more informative to investigate the neural substrate of memory subfunctions in earlier stages (e.g. MCI population) whereas subregional atrophy pattern might prove more useful in later stages of disease development (e.g. AD population). The finding that tau burden (composite MTL-tau) correlates with memory scores (ADAS) in MCI was promising that this population might be suitable for studying specialised sub-function of memory of each MTL subfield in. At MCI stage, the impairment is more likely to be domain-specific thus methods such as event-based modelling to track NFT distribution in each MTL substructure combined with more specific tests for memory subfunctions might potentially allow us to probe structural correlate of memory subfunctions.

According to cognitive reserve theory, given similar level of brain damage, people with better cognitive reserve have less severe the symptoms (Möller et al., 2013). Möller et al. (2013) proposed that early-onset AD patients might have more cognitive reserve, explaining the finding of more widespread atrophy in the presence of similar performance on the MMSE. Our finding somewhat contradicts this notion. In our study, despite comparable volume loss between EOMCI and LOMCI, EOMCI group had worse memory performance (ADAS scores). Alternative interpretation would be that higher cognitive reserve in late onset group delayed the onset of clinical symptoms in spite of comparable pathological burden. Further research is needed to investigate the role of cognitive reserve in onset of AD symptoms.

Our study has numerous strengths but also notable limitations. High resolution T2-weighted imaging allowed more accurate visualisation of subfields which are less visible on T1-weighted images (Xie et al., 2019). Moreover, the ASHS segmentation method used in this study has been well-validated and developed in collaboration with a neuroanatomist (Berron et al., 2017). Focusing on the typical amnestic subtype of AD minimised variant-related heterogeneity and higher prevalence of this variant maximised the sample size. Validating positive AD pathology in the patient group and AD negativity in control groups using biomarkers allowed for better patient-control contrast. We also used a more liberal cut-off age of 70 to partition early and late onset groups. This is done to avoid erroneously assigning early onset patients to the late onset

group as the age at onset is an estimation. Future studies should explore using different age cut-offs. Despite our best effort, our study inevitably suffered from a small sample size like many other studies. However, group differences were consistently observed. Exclusive focus on amnestic variant and only including AD negative healthy controls might have reduced heterogeneity and improved the statistical power.

Nevertheless, our study contributed a novel finding that MTL subregional atrophy in EOAD and LOAD of amnestic type share similar pattern. This insight will contribute to designing research studies and clinical trials in AD (Reitz et al., 2020). Moreover, selective and predictable subregional neurodegeneration in AD will allow identification of regional correlates of memory sub-functions. The benefit of such research is multi-fold as it advances our understanding of memory function which in turn could be utilised to develop more sophisticated clinical diagnostic tests for AD. Furthermore, a more complete map of the clinical symptoms and regional distribution of tau will also advance our understanding of the neuropathological framework underlying the clinical manifestations in AD (Ossenkoppele et al., 2015).

References

American Psychiatric Association. (2013). Diagnostic and statistical manual of mental disorders (5th ed.). https://doi.org/10.1176/appi.books.9780890425596

Amador-Ortiz, C., Lin, W. L., Ahmed, Z., Personett, D., Davies, P., Duara, R., Graff-Radford, N. R., Hutton, M. L., & Dickson, D. W. (2007). TDP-43 immunoreactivity in hippocampal sclerosis and Alzheimer's disease. *Annals of neurology*, *61*(5), 435-445. https://doi.org/10.1002/ana.21154

Ayodele, T., Rogaeva, E., Kurup, J. T., Beecham, G., & Reitz, C. (2021). Early-Onset Alzheimer's Disease: What Is Missing in Research? *Current Neurology and Neuroscience Reports*, *21*(2), 4. https://doi.org/10.1007/s11910-020-01090-y

Baker, S. L., Maass, A., & Jagust, W. J. (2017). Considerations and code for partial volume correcting [(18)F]-AV-1451 tau PET data. *Data Brief*, *15*, 648-657. https://doi.org/10.1016/j.dib.2017.10.024

Bateman, R. J., Aisen, P. S., De Strooper, B., Fox, N. C., Lemere, C. A., Ringman, J. M., Salloway, S., Sperling, R. A., Windisch, M., & Xiong, C. (2011). Autosomal-dominant Alzheimer's disease: a review and proposal for the prevention of Alzheimer's disease. *Alzheimer's Research & Therapy*, *3*(1), 1. https://doi.org/10.1186/alzrt59

Berron, D., Vieweg, P., Hochkeppler, A., Pluta, J. B., Ding, S. L., Maass, A., Luther, A., Xie, L., Das, S. R., Wolk, D. A., Wolbers, T., Yushkevich, P. A., Düzel, E., & Wisse, L. E. M. (2017). A protocol for manual segmentation of medial temporal lobe subregions in 7 Tesla MRI. *NeuroImage. Clinical*, *15*, 466-482. https://doi.org/10.1016/j.nicl.2017.05.022

Berron, D., Vogel, J. W., Insel, P. S., Pereira, J. B., Xie, L., Wisse, L. E. M., Yushkevich, P. A., Palmqvist, S., Mattsson-Carlgren, N., Stomrud, E., Smith, R., Strandberg, O., & Hansson, O. (2021). Early stages of tau pathology and its associations with functional connectivity, atrophy and memory. *Brain*. https://doi.org/10.1093/brain/awab114

Bertens, D., Tijms, B. M., Scheltens, P., Teunissen, C. E., & Visser, P. J. (2017). Unbiased estimates of cerebrospinal fluid β-amyloid 1-42 cutoffs in a large memory clinic population. *Alzheimers Res Ther*, *9*(1), 8. https://doi.org/10.1186/s13195-016-0233-7

Bobinski, M., Wegiel, J., Tarnawski, M., Bobinski, M., Reisberg, B., de Leon, M. J., Miller, D. C., & Wisniewski, H. M. (1997). Relationships between regional neuronal loss and neurofibrillary changes in the hippocampal formation and duration and severity of Alzheimer disease. *J Neuropathol Exp Neurol*, *56*(4), 414-420. https://doi.org/10.1097/00005072-199704000-00010

Braak, H., Alafuzoff, I., Arzberger, T., Kretzschmar, H., & Del Tredici, K. (2006). Staging of Alzheimer disease-associated neurofibrillary pathology using paraffin sections and immunocytochemistry. *Acta Neuropathol*, *112*(4), 389-404. https://doi.org/10.1007/s00401-006-0127-z

Braak, H., & Braak, E. (1991). Neuropathological stageing of Alzheimer-related changes. *Acta Neuropathologica*, *82*(4), 239-259. https://doi.org/10.1007/BF00308809

Braak, H., & Braak, E. (1995). Staging of alzheimer's disease-related neurofibrillary changes. *Neurobiology of Aging*, *16*(3), 271-278. https://doi.org/https://doi.org/10.1016/0197-4580(95)00021-6

Braak, H., & Del Tredici, K. (2020). From the Entorhinal Region via the Prosubiculum to the Dentate Fascia: Alzheimer Disease-Related Neurofibrillary Changes in the Temporal Allocortex. *J Neuropathol Exp Neurol*, *79*(2), 163-175. https://doi.org/10.1093/jnen/nlz123

Cavedo, E., Pievani, M., Boccardi, M., Galluzzi, S., Bocchetta, M., Bonetti, M., Thompson, P. M., & Frisoni, G. B. (2014). Medial temporal atrophy in early and late-onset Alzheimer's disease. *Neurobiology of Aging*, *35*(9), 2004-2012. https://doi.org/10.1016/j.neurobiolaging.2014.03.009

Chételat, G., Fouquet, M., Kalpouzos, G., Denghien, I., De la Sayette, V., Viader, F., Mézenge, F., Landeau, B., Baron, J. C., Eustache, F., & Desgranges, B. (2008). Three-dimensional surface mapping of hippocampal atrophy progression from MCI to AD and over normal aging as assessed using voxel-based morphometry. *Neuropsychologia*, *46*(6), 1721-1731. https://doi.org/10.1016/j.neuropsychologia.2007.11.037

Daugherty, A. M., Bender, A. R., Raz, N., & Ofen, N. (2016). Age differences in hippocampal subfield volumes from childhood to late adulthood. *Hippocampus*, *26*(2), 220-228. https://doi.org/10.1002/hipo.22517

Davies, P., & Terry, R. D. (1981). Cortical somatostatin-like immunoreactivity in cases of Alzheimer's disease and senile dementia of the Alzheimer type. *Neurobiology of Aging*, *2*(1), 9-14.

de Flores, R., La Joie, R., & Chételat, G. (2015). Structural imaging of hippocampal subfields in healthy aging and Alzheimer's disease. *Neuroscience*, *309*, 29-50. https://doi.org/https://doi.org/10.1016/j.neuroscience.2015.08.033

de Flores, R., La Joie, R., Landeau, B., Perrotin, A., Mézenge, F., de La Sayette, V., Eustache, F., Desgranges, B., & Chételat, G. (2015a). Effects of age and Alzheimer's disease on hippocampal subfields. *Human Brain Mapping*, *36*(2), 463-474. https://doi.org/https://doi.org/10.1002/hbm.22640

de Flores, R., La Joie, R., Landeau, B., Perrotin, A., Mézenge, F., de La Sayette, V., Eustache, F., Desgranges, B., & Chételat, G. (2015b). Effects of age and Alzheimer's disease on hippocampal subfields: Comparison between manual and FreeSurfer volumetry. *Human Brain Mapping*, *36*(2), 463-474. https://doi.org/10.1002/hbm.22640

de Flores, R., Wisse, L. E. M., Das, S. R., Xie, L., McMillan, C. T., Trojanowski, J. Q., Robinson, J. L., Grossman, M., Lee, E., Irwin, D. J., Yushkevich, P. A., & Wolk, D. A. (2020). Contribution of mixed pathology to medial temporal lobe atrophy in Alzheimer's disease. *Alzheimer's & dementia : the journal of the Alzheimer's Association*, *16*(6), 843-852. https://doi.org/10.1002/alz.12079

De Souza, L. C., Chupin, M., Lamari, F., Jardel, C., Leclercq, D., Colliot, O., Lehéricy, S., Dubois, B., & Sarazin, M. (2012). CSF tau markers are correlated with hippocampal volume in Alzheimer's disease. *Neurobiology of Aging*, *33*(7), 1253-1257.

Ferreira, D., Nordberg, A., & Westman, E. (2020). Biological subtypes of Alzheimer disease: A systematic review and meta-analysis. *Neurology*, *94*(10), 436-448. https://doi.org/10.1212/wnl.0000000000009058

Folstein, M. F., Folstein, S. E., & McHugh, P. R. (1975). "Mini-mental state": a practical method for grading the cognitive state of patients for the clinician. *Journal of psychiatric research*, *12*(3), 189-198.

Frisoni, G., Testa, C., Sabattoli, F., Beltramello, A., Soininen, H., & Laakso, M. (2005). Structural correlates of early and late onset Alzheimer's disease: voxel based morphometric study. *Journal of Neurology, Neurosurgery & Psychiatry*, *76*(1), 112-114.

Genon, S., Reid, A., Langner, R., Amunts, K., & Eickhoff, S. B. (2018). How to Characterize the Function of a Brain Region. *Trends in Cognitive Sciences*, *22*(4), 350-364. https://doi.org/https://doi.org/10.1016/j.tics.2018.01.010

Grinberg, L. T., Petersen, C., Nolan, A. L., Resende, E. d. P. F., Miller, Z. A., Spina, S., Miller, B. L., Rabinovici, G. D., & Seeley, W. W. (2020). Examining early-onset Alzheimer's disease (EOAD) and late-onset Alzheimer's disease to understand the neuropathological substract of typical and atypical AD. *Alzheimer's & Dementia*, *16*(S5), e041616. https://doi.org/https://doi.org/10.1002/alz.041616

Hanseeuw, B., Van Leemput, K., Kavec, M., Grandin, C., Seron, X., & Ivanoiu, A. (2011). Mild cognitive impairment: differential atrophy in the hippocampal subfields. *American Journal of Neuroradiology*, *32*(9), 1658-1661.

Harvey, R. J., Skelton-Robinson, M., & Rossor, M. N. (2003). The prevalence and causes of dementia in people under the age of 65 years. *Journal of Neurology, Neurosurgery & Psychiatry*, *74*(9), 1206-1209. https://doi.org/10.1136/jnnp.74.9.1206

Holland, D., Desikan, R. S., Dale, A. M., & McEvoy, L. K. (2012). Rates of decline in Alzheimer disease decrease with age. *PLOS ONE*, *7*(8), e42325. https://doi.org/10.1371/journal.pone.0042325

Iglesias, J. E., Augustinack, J. C., Nguyen, K., Player, C. M., Player, A., Wright, M., Roy, N., Frosch, M. P., McKee, A. C., Wald, L. L., Fischl, B., & Van Leemput, K. (2015). A computational atlas of the hippocampal formation using ex vivo, ultra-high resolution MRI: Application to adaptive segmentation of in vivo MRI. *Neuroimage*, *115*, 117-137. https://doi.org/10.1016/j.neuroimage.2015.04.042

Ingelsson, M., Fukumoto, H., Newell, K., Growdon, J., Hedley–Whyte, E., Frosch, M., Albert, M., Hyman, B., & Irizarry, M. (2004). Early Aβ accumulation and progressive synaptic loss, gliosis, and tangle formation in AD brain. *Neurology*, *62*(6), 925-931.

Jack, C., Dickson, D., Parisi, J., Xu, Y., Cha, R., O'brien, P., Edland, S., Smith, G., Boeve, B., & Tangalos, E. (2002). Antemortem MRI findings correlate with hippocampal neuropathology in typical aging and dementia. *Neurology*, *58*(5), 750-757.

Jack, C. R., Jr., Bennett, D. A., Blennow, K., Carrillo, M. C., Dunn, B., Haeberlein, S. B., Holtzman, D. M., Jagust, W., Jessen, F., Karlawish, J., Liu, E., Molinuevo, J. L., Montine, T., Phelps, C., Rankin, K. P., Rowe, C. C., Scheltens, P., Siemers, E., Snyder, H. M., & Sperling, R. (2018). NIA-AA Research Framework: Toward a biological definition of Alzheimer's disease. *Alzheimer's & dementia : the journal of the Alzheimer's Association*, *14*(4), 535-562. https://doi.org/10.1016/j.jalz.2018.02.018

Jack, C. R., Jr., & Holtzman, D. M. (2013). Biomarker modeling of Alzheimer's disease. *Neuron*, *80*(6), 1347-1358. https://doi.org/10.1016/j.neuron.2013.12.003

James, B. D., Wilson, R. S., Boyle, P. A., Trojanowski, J. Q., Bennett, D. A., & Schneider, J. A. (2016). TDP-43 stage, mixed pathologies, and clinical Alzheimer's-type dementia. *Brain*, *139*(11), 2983-2993. https://doi.org/10.1093/brain/aww224

Josephs, K. A., Dickson, D. W., Tosakulwong, N., Weigand, S. D., Murray, M. E., Petrucelli, L., Liesinger, A. M., Senjem, M. L., Spychalla, A. J., Knopman, D. S., Parisi, J. E., Petersen, R. C., Jack, C. R., Jr., & Whitwell, J. L. (2017). Rates of hippocampal atrophy and presence of post-mortem TDP-43 in patients with Alzheimer's disease: a longitudinal retrospective study. *The Lancet. Neurology*, *16*(11), 917-924. https://doi.org/10.1016/s1474-4422(17)30284-3

Josephs, K. A., Whitwell, J. L., Tosakulwong, N., Weigand, S. D., Murray, M. E., Liesinger, A. M., Petrucelli, L., Senjem, M. L., Ivnik, R. J., Parisi, J. E., Petersen, R. C., & Dickson, D.

W. (2015). TAR DNA-binding protein 43 and pathological subtype of Alzheimer's disease impact clinical features. *Annals of neurology*, *78*(5), 697-709. https://doi.org/10.1002/ana.24493

Kirwan, C. B., Wixted, J. T., & Squire, L. R. (2008). Activity in the Medial Temporal Lobe Predicts Memory Strength, Whereas Activity in the Prefrontal Cortex Predicts Recollection. *The Journal of Neuroscience*, *28*(42), 10541-10548. https://doi.org/10.1523/jneurosci.3456-08.2008

Koedam, E. L. G. E., Lauffer, V., van der Vlies, A. E., van der Flier, W. M., Scheltens, P., & Pijnenburg, Y. A. L. (2010). Early-Versus Late-Onset Alzheimer's Disease: More than Age Alone. *Journal of Alzheimer's Disease*, *19*, 1401-1408. https://doi.org/10.3233/JAD-2010-1337

Kuwabara, H., Comley, R. A., Borroni, E., Honer, M., Kitmiller, K., Roberts, J., Gapasin, L., Mathur, A., Klein, G., & Wong, D. F. (2018). Evaluation of (18)F-RO-948 PET for Quantitative Assessment of Tau Accumulation in the Human Brain. *J Nucl Med*, *59*(12), 1877-1884. https://doi.org/10.2967/jnumed.118.214437

La Joie, R., Fouquet, M., Mézenge, F., Landeau, B., Villain, N., Mevel, K., Pélerin, A., Eustache, F., Desgranges, B., & Chételat, G. (2010). Differential effect of age on hippocampal subfields assessed using a new high-resolution 3T MR sequence. *Neuroimage*, *53*(2), 506-514. https://doi.org/10.1016/j.neuroimage.2010.06.024

La Joie, R., Perrotin, A., de La Sayette, V., Egret, S., Doeuvre, L., Belliard, S., Eustache, F., Desgranges, B., & Chételat, G. (2013). Hippocampal subfield volumetry in mild cognitive impairment, Alzheimer's disease and semantic dementia. *NeuroImage. Clinical*, *3*, 155-162. https://doi.org/10.1016/j.nicl.2013.08.007

Ledergerber, D., & Moser, E. I. (2017). Memory Retrieval: Taking the Route via Subiculum. *Current Biology*, *27*(22), R1225-R1227. https://doi.org/https://doi.org/10.1016/j.cub.2017.09.042

Leutgeb, J. K., Leutgeb, S., Moser, M. B., & Moser, E. I. (2007). Pattern separation in the dentate gyrus and CA3 of the hippocampus. *Science*, *315*(5814), 961-966. https://doi.org/10.1126/science.1135801

Leuzy, A., Smith, R., Ossenkoppele, R., Santillo, A., Borroni, E., Klein, G., Ohlsson, T., Jögi, J., Palmqvist, S., Mattsson-Carlgren, N., Strandberg, O., Stomrud, E., & Hansson, O. (2020). Diagnostic Performance of RO948 F 18 Tau Positron Emission Tomography in the Differentiation of Alzheimer Disease From Other Neurodegenerative Disorders. *JAMA Neurology*, *77*(8), 955-965. https://doi.org/10.1001/jamaneurol.2020.0989

Lindberg, O., Mårtensson, G., Stomrud, E., Palmqvist, S., Wahlund, L. O., Westman, E., & Hansson, O. (2017). Atrophy of the Posterior Subiculum Is Associated with Memory Impairment, Tau- and Aβ Pathology in Non-demented Individuals. *Frontiers in aging neuroscience*, *9*, 306. https://doi.org/10.3389/fnagi.2017.00306

Malykhin, N. V., Huang, Y., Hrybouski, S., & Olsen, F. (2017). Differential vulnerability of hippocampal subfields and anteroposterior hippocampal subregions in healthy cognitive aging. *Neurobiol Aging*, *59*, 121-134. https://doi.org/10.1016/j.neurobiolaging.2017.08.001

Manns, J. R., & Eichenbaum, H. (2007). 3.33 - Evolution of the Hippocampus. In J. H. Kaas (Ed.), *Evolution of Nervous Systems* (pp. 465-489). Academic Press. https://doi.org/https://doi.org/10.1016/B0-12-370878-8/00086-0

Maruszak, A., & Thuret, S. (2014). Why looking at the whole hippocampus is not enough-a critical role for anteroposterior axis, subfield and activation analyses to enhance

predictive value of hippocampal changes for Alzheimer's disease diagnosis. *Frontiers in cellular neuroscience*, *8*, 95-95. https://doi.org/10.3389/fncel.2014.00095

McKhann, G., Drachman, D., Folstein, M., Katzman, R., Price, D., & Stadlan, E. M. (1984). Clinical diagnosis of Alzheimer's disease: Report of the NINCDS-ADRDA Work Group* under the auspices of Department of Health and Human Services Task Force on Alzheimer's Disease. *Neurology*, *34*(7), 939-939.

Mendez, M. F. (2012). Early-onset Alzheimer's Disease: Nonamnestic Subtypes and Type 2 AD. *Archives of Medical Research*, *43*(8), 677-685. https://doi.org/https://doi.org/10.1016/j.arcmed.2012.11.009

Mendez, M. F. (2017). Early-Onset Alzheimer Disease. *Neurol Clin*, *35*(2), 263-281. https://doi.org/10.1016/j.ncl.2017.01.005

Milner, B. (2005). The medial temporal-lobe amnesic syndrome. *Psychiatric Clinics*, *28*(3), 599-611.

Möller, C., Vrenken, H., Jiskoot, L., Versteeg, A., Barkhof, F., Scheltens, P., & van der Flier, W. M. (2013). Different patterns of gray matter atrophy in early- and late-onset Alzheimer's disease. *Neurobiology of Aging*, *34*(8), 2014-2022. https://doi.org/https://doi.org/10.1016/j.neurobiolaging.2013.02.013

Mueller, S. G., Chao, L. L., Berman, B., & Weiner, M. W. (2011). Evidence for functional specialization of hippocampal subfields detected by MR subfield volumetry on high resolution images at 4T. *Neuroimage*, *56*(3), 851-857. https://doi.org/https://doi.org/10.1016/j.neuroimage.2011.03.028

Mueller, S. G., Yushkevich, P. A., Das, S., Wang, L., Van Leemput, K., Iglesias, J. E., Alpert, K., Mezher, A., Ng, P., Paz, K., Weiner, M. W., & Alzheimer's Disease Neuroimaging, I. (2017). Systematic comparison of different techniques to measure hippocampal subfield volumes in ADNI2. *NeuroImage. Clinical*, *17*, 1006-1018. https://doi.org/10.1016/j.nicl.2017.12.036

Murray, M. E., Graff-Radford, N. R., Ross, O. A., Petersen, R. C., Duara, R., & Dickson, D. W. (2011). Neuropathologically defined subtypes of Alzheimer's disease with distinct clinical characteristics: a retrospective study. *The Lancet Neurology*, *10*(9), 785-796. https://doi.org/https://doi.org/10.1016/S1474-4422(11)70156-9

Nelson, P., Smith, C., Abner, E., Wilfred, B., Wang, W.-X., Neltner, J., Baker, M., Fardo, D., Kryscio, R., Scheff, S., Jicha, G., Jellinger, K., Van Eldik, L., & Schmitt, F. (2013). Hippocampal sclerosis of aging, a prevalent and high-morbidity brain disease. *Acta Neuropathologica*, *126*. https://doi.org/10.1007/s00401-013-1154-1

Nelson, P. T., Braak, H., & Markesbery, W. R. (2009). Neuropathology and cognitive impairment in Alzheimer disease: a complex but coherent relationship. *J Neuropathol Exp Neurol*, *68*(1), 1-14. https://doi.org/10.1097/NEN.0b013e3181919a48

Nelson, P. T., Dickson, D. W., Trojanowski, J. Q., Jack, C. R., Boyle, P. A., Arfanakis, K., Rademakers, R., Alafuzoff, I., Attems, J., Brayne, C., Coyle-Gilchrist, I. T. S., Chui, H. C., Fardo, D. W., Flanagan, M. E., Halliday, G., Hokkanen, S. R. K., Hunter, S., Jicha, G. A., Katsumata, Y., Kawas, C. H., Keene, C. D., Kovacs, G. G., Kukull, W. A., Levey, A. I., Makkinejad, N., Montine, T. J., Murayama, S., Murray, M. E., Nag, S., Rissman, R. A., Seeley, W. W., Sperling, R. A., White Iii, C. L., Yu, L., & Schneider, J. A. (2019). Limbic-predominant age-related TDP-43 encephalopathy (LATE): consensus working group report. *Brain*, *142*(6), 1503-1527. https://doi.org/10.1093/brain/awz099

Ohm, T. G. (2007). The dentate gyrus in Alzheimer's disease. In H. E. Scharfman (Ed.), *Progress in Brain Research* (Vol. 163, pp. 723-740). Elsevier. https://doi.org/https://doi.org/10.1016/S0079-6123(07)63039-8

Ossenkoppele, R., Cohn-Sheehy, B. I., La Joie, R., Vogel, J. W., Möller, C., Lehmann, M., van Berckel, B. N. M., Seeley, W. W., Pijnenburg, Y. A., Gorno-Tempini, M. L., Kramer, J. H., Barkhof, F., Rosen, H. J., van der Flier, W. M., Jagust, W. J., Miller, B. L., Scheltens, P., & Rabinovici, G. D. (2015). Atrophy patterns in early clinical stages across distinct phenotypes of Alzheimer's disease. *Human Brain Mapping*, *36*(11), 4421-4437. https://doi.org/https://doi.org/10.1002/hbm.22927

Petersen, C., Nolan, A. L., de Paula França Resende, E., Miller, Z., Ehrenberg, A. J., Gorno-Tempini, M. L., Rosen, H. J., Kramer, J. H., Spina, S., Rabinovici, G. D., Miller, B. L., Seeley, W. W., Heinsen, H., & Grinberg, L. T. (2019). Alzheimer's disease clinical variants show distinct regional patterns of neurofibrillary tangle accumulation. *Acta Neuropathol*, *138*(4), 597-612. https://doi.org/10.1007/s00401-019-02036-6

Petersen, R. C. (2004). Mild cognitive impairment as a diagnostic entity. *J Intern Med*, *256*(3), 183-194. https://doi.org/10.1111/j.1365-2796.2004.01388.x

Petersen, R. C., Smith, G. E., Waring, S. C., Ivnik, R. J., Tangalos, E. G., & Kokmen, E. (1999). Mild cognitive impairment: clinical characterization and outcome. *Arch Neurol*, *56*(3), 303-308. https://doi.org/10.1001/archneur.56.3.303

Pluta, J., Yushkevich, P., Das, S., & Wolk, D. (2012). In vivo analysis of hippocampal subfield atrophy in mild cognitive impairment via semi-automatic segmentation of T2-weighted MRI. *Journal of Alzheimer's Disease*, *31*(1), 85-99.

Raji, C. A., Lopez, O. L., Kuller, L. H., Carmichael, O. T., & Becker, J. T. (2009). Age, Alzheimer disease, and brain structure. *Neurology*, *73*(22), 1899-1905. https://doi.org/10.1212/WNL.0b013e3181c3f293

Raz, N., Lindenberger, U., Rodrigue, K. M., Kennedy, K. M., Head, D., Williamson, A., Dahle, C., Gerstorf, D., & Acker, J. D. (2005). Regional brain changes in aging healthy adults: general trends, individual differences and modifiers. *Cerebral cortex (New York, N.Y. : 1991)*, *15*(11), 1676-1689. https://doi.org/10.1093/cercor/bhi044

Reitz, C., Rogaeva, E., & Beecham, G. W. (2020). Late-onset vs nonmendelian early-onset Alzheimer disease: A distinction without a difference? *Neurol Genet*, *6*(5), e512. https://doi.org/10.1212/nxg.0000000000000512

Rosen, W. G., Mohs, R. C., & Davis, K. L. (1984). A new rating scale for Alzheimer's disease. *Am J Psychiatry*, *141*(11), 1356-1364. https://doi.org/10.1176/ajp.141.11.1356

Rosene, D. L., & Van Hoesen, G. W. (1987). The Hippocampal Formation of the Primate Brain. In E. G. Jones & A. Peters (Eds.), *Cerebral Cortex: Further Aspects of Cortical Function, Including Hippocampus* (pp. 345-456). Springer US. https://doi.org/10.1007/978-1-4615-6616-8_9

Rossor, M. N., Fox, N. C., Mummery, C. J., Schott, J. M., & Warren, J. D. (2010). The diagnosis of young-onset dementia. *The Lancet Neurology*, *9*(8), 793-806. https://doi.org/10.1016/S1474-4422(10)70159-9

Rugg, M. D., & Vilberg, K. L. (2013). Brain networks underlying episodic memory retrieval. *Current Opinion in Neurobiology*, *23*(2), 255-260. https://doi.org/https://doi.org/10.1016/j.conb.2012.11.005

Schöll, M., Ossenkoppele, R., Strandberg, O., Palmqvist, S., study, T. S. B., Jögi, J., Ohlsson, T., Smith, R., & Hansson, O. (2017). Distinct 18F-AV-1451 tau PET retention patterns in

early- and late-onset Alzheimer's disease. *Brain*, *140*(9), 2286-2294. https://doi.org/10.1093/brain/awx171

Shiino, A., Watanabe, T., Kitagawa, T., Kotani, E., Takahashi, J., Morikawa, S., & Akiguchi, I. (2008). Different atrophic patterns in early- and late-onset Alzheimer's disease and evaluation of clinical utility of a method of regional z-score analysis using voxel-based morphometry. *Dement Geriatr Cogn Disord*, *26*(2), 175-186. https://doi.org/10.1159/000151241

Small, S. A. (2014). Isolating pathogenic mechanisms embedded within the hippocampal circuit through regional vulnerability. *Neuron*, *84*(1), 32-39. https://doi.org/10.1016/j.neuron.2014.08.030

Small, S. A., Tsai, W. Y., DeLaPaz, R., Mayeux, R., & Stern, Y. (2002). Imaging hippocampal function across the human life span: is memory decline normal or not? *Annals of neurology*, *51*(3), 290-295. https://doi.org/10.1002/ana.10105

Spina, S., La Joie, R., Petersen, C., Nolan, A. L., Cuevas, D., Cosme, C., Hepker, M., Hwang, J. H., Miller, Z. A., Huang, E. J., Karydas, A. M., Grant, H., Boxer, A. L., Gorno-Tempini, M. L., Rosen, H. J., Kramer, J. H., Miller, B. L., Seeley, W. W., Rabinovici, G. D., & Grinberg, L. T. (2021). Comorbid neuropathological diagnoses in early versus late-onset Alzheimer's disease. *Brain*. https://doi.org/10.1093/brain/awab099

Squire, L. R. (2009). The Legacy of Patient H.M. for Neuroscience. *Neuron*, *61*(1), 6-9. https://doi.org/https://doi.org/10.1016/j.neuron.2008.12.023

Tardif, C. L., Devenyi, G. A., Amaral, R. S. C., Pelleieux, S., Poirier, J., Rosa-Neto, P., Breitner, J., & Chakravarty, M. M. (2018). Regionally specific changes in the hippocampal circuitry accompany progression of cerebrospinal fluid biomarkers in preclinical Alzheimer's disease. *Hum Brain Mapp*, *39*(2), 971-984. https://doi.org/10.1002/hbm.23897

Tellechea, P., Pujol, N., Esteve-Belloch, P., Echeveste, B., García-Eulate, M. R., Arbizu, J., & Riverol, M. (2018). Early- and late-onset Alzheimer disease: Are they the same entity? [10.1016/j.nrleng.2015.08.009]. *Neurología (English Edition)*, *33*(4), 244-253. https://doi.org/10.1016/j.nrleng.2015.08.009

Travis, S. G., Huang, Y., Fujiwara, E., Radomski, A., Olsen, F., Carter, R., Seres, P., & Malykhin, N. V. (2014). High field structural MRI reveals specific episodic memory correlates in the subfields of the hippocampus. *Neuropsychologia*, *53*, 233-245. https://doi.org/10.1016/j.neuropsychologia.2013.11.016

Tulving, E. (2002). Episodic Memory: From Mind to Brain. *Annual Review of Psychology*, *53*(1), 1-25. https://doi.org/10.1146/annurev.psych.53.100901.135114

Vago, D. R., Wallenstein, G. V., & Morris, L. S. (2014). Hippocampus. In M. J. Aminoff & R. B. Daroff (Eds.), *Encyclopedia of the Neurological Sciences (Second Edition)* (pp. 566-570). Academic Press. https://doi.org/https://doi.org/10.1016/B978-0-12-385157-4.01151-9

van der Flier, W. M., Pijnenburg, Y. A. L., Fox, N. C., & Scheltens, P. (2011). Early-onset versus late-onset Alzheimer's disease: the case of the missing APOE ɛ4 allele. *The Lancet Neurology*, *10*(3), 280-288. https://doi.org/10.1016/S1474-4422(10)70306-9

West, M. J., Coleman, P. D., Flood, D. G., & Troncoso, J. C. (1994). Differences in the pattern of hippocampal neuronal loss in normal ageing and Alzheimer's disease. *Lancet*, *344*(8925), 769-772. https://doi.org/10.1016/s0140-6736(94)92338-8

Whitwell, J. L., Josephs, K. A., Murray, M. E., Kantarci, K., Przybelski, S., Weigand, S., Vemuri, P., Senjem, M., Parisi, J. E., & Knopman, D. S. (2008). MRI correlates of neurofibrillary

tangle pathology at autopsy: a voxel-based morphometry study. *Neurology*, *71*(10), 743-749.

Whitwell, J. L., Przybelski, S. A., Weigand, S. D., Knopman, D. S., Boeve, B. F., Petersen, R. C., & Jack, C. R., Jr. (2007). 3D maps from multiple MRI illustrate changing atrophy patterns as subjects progress from mild cognitive impairment to Alzheimer's disease. *Brain*, *130*(Pt 7), 1777-1786. https://doi.org/10.1093/brain/awm112

Wisse, L. E. M., Biessels, G. J., Heringa, S. M., Kuijf, H. J., Koek, D. L., Luijten, P. R., & Geerlings, M. I. (2014). Hippocampal subfield volumes at 7T in early Alzheimer's disease and normal aging. *Neurobiology of Aging*, *35*(9), 2039-2045. https://doi.org/https://doi.org/10.1016/j.neurobiolaging.2014.02.021

Wolk, D. A., Das, S. R., Mueller, S. G., Weiner, M. W., & Yushkevich, P. A. (2017). Medial temporal lobe subregional morphometry using high resolution MRI in Alzheimer's disease. *Neurobiol Aging*, *49*, 204-213. https://doi.org/10.1016/j.neurobiolaging.2016.09.011

Xie, L., Wisse, L. E. M., Pluta, J., de Flores, R., Piskin, V., Manjón, J. V., Wang, H., Das, S. R., Ding, S. L., Wolk, D. A., & Yushkevich, P. A. (2019). Automated segmentation of medial temporal lobe subregions on in vivo T1-weighted MRI in early stages of Alzheimer's disease. *Hum Brain Mapp*, *40*(12), 3431-3451. https://doi.org/10.1002/hbm.24607

Yushkevich, P. A., Pluta, J. B., Wang, H., Xie, L., Ding, S. L., Gertje, E. C., Mancuso, L., Kliot, D., Das, S. R., & Wolk, D. A. (2015). Automated volumetry and regional thickness analysis of hippocampal subfields and medial temporal cortical structures in mild cognitive impairment. *Human Brain Mapping*, *36*(1), 258-287.